Title
Excitation functions of some deuteron-induced nuclear reactions on Al

Journal
Radiochimica Acta, 109(10)

ISSN
0033-8230

Authors
Uddin, M Shuza
Basunia, M Shamsuzzoha
Qaim, Syed M

Publication Date
2021-10-01

DOI
10.1515/ract-2021-1065

Excitation functions of some deuteron-induced nuclear reactions on Al

M. Shuza Uddin [1,2*], M. Shamsuzzoha Basunia[1], Syed M. Qaim[3]

[1]*Nuclear Science Division, Lawrence Berkeley National Laboratory, Berkeley, California 94720, USA*

[2] *Tandem Accelerator Facilities, INST, Atomic Energy Research Establishment, Savar, Dhaka, Bangladesh*

[3] *Institut für Neurowissenschaften und Medizin, INM-5: Nuklearchemie, Forschungszentrum Jülich GmbH, D-52425 Jülich, Germany*

Abstract

Excitation functions of the reactions ^{27}Al(d,αp)^{24}Na, ^{27}Al(d,2p)^{27}Mg and ^{27}Al(d,p)^{28}Al were measured by the activation technique up to deuteron energies of 37 MeV. The available experimental databases of the reaction products ^{27}Mg and ^{28}Al were extended and compared with the nuclear model calculations based on the code TALYS-1.8. Our measured data are reproduced well by the model calculations after adjustment of a few free input parameters. The cross-section ratio of the (d,αp) to (d,2p) process as a function of projectile energy was deduced from the measured data, and the result is interpreted in terms of competition between proton and an α-particle.

Keywords: ^{27}Al+d process, Activation technique, Cross section, Cross-section ratio, Excitation function, TALYS calculation.

1 Introduction

Deuteron-induced nuclear reactions in the low energy region are of considerable significance in nuclear research, both fundamental and application-oriented. Aluminium is an important structural element utilized in nuclear technology. The deuteron-induced activation cross sections on Al are of interest for proper estimation of radioactivity as well as for the safety in design and management of the International Fusion Materials Irradiation Facility (IFMIF) [1,2]. The reactions ^{27}Al(d,2p)^{27}Mg and ^{27}Al(d,p)^{28}Al are of great interest in astrophysics studies [3]. For understanding the mechanisms of deuteron-induced reactions on Al and

* Author for correspondence, E-mail: md.shuzauddin@yahoo.com

validation of the prediction codes, a detailed accurate production data for various radionuclides are needed.

The $^{27}Al(d,x)^{24}Na$ reaction is used for monitoring the deuteron beam in fundamental research and isotope production. Hermanne et al. [4] reported evaluated data for the above reaction up to 80 MeV. Furthermore, a very detailed analysis of this reaction up to 20 MeV, consisting of estimation of direct, precompound and compound components, was reported by Bém et al. [5]. In contrast, the data for two other reactions, viz. $^{27}Al(d,2p)^{27}Mg$ and $^{27}Al(d,p)^{28}Al$, are somewhat discrepant [5-11], and additional measurements and intercomparisons were considered necessary. The aim of this work was therefore to extend the databases of those two reactions up to 37 MeV and to compare the results with nuclear model calculations. Furthermore, the data for the formation of ^{24}Na and ^{27}Mg, which involve the emission of two charged particles, should be compared and qualitatively discussed.

2 Experimental techniques

2.1 Sample preparation and irradiations

Cross sections of deuteron induced reactions on ^{27}Al were obtained as subsidiary results in stacked-foil activation experiments on some medically related radionuclides. Two stacks were prepared with Al, Cu and Ti foils of natural isotopic composition, together with several other thin samples. Al foils of 50 μm thickness (supplied by Good Fellow; chemical purity: 99.0 %) were used for measuring short-lived products. Thin foils of Cu and Ti (supplied by Good Fellow; purity: Cu (99.9 %); Ti (>99.6 %), thickness of both Cu and Ti foils: 25 μm) were used as beam monitor as well as beam energy degrader along the stack. All the foils were cut in circular discs with a diameter of 13 mm.

One stack was irradiated with deuterons of primary energy of 35 and the other with 40 MeV at the 88-inch cyclotron, Lawrence Berkeley National Laboratory (LBNL), USA, for periods of 30 and 45 min, respectively. During the irradiation, the beam current was kept constant at about 100 nA.

2.2 Beam characterization

The extracted beam at the 88-inch cyclotron at LBNL is well characterized. Nevertheless, the primary energy of the incident deuterons was checked by the decay-rate ratio of $^{63}Zn/^{62}Zn$ formed in the same Cu monitor foil (25 μm thick) mounted in front of the stack. For this purpose, the count rates of the two products, namely ^{63}Zn ($T_{½}$ = 38.47 min) and ^{62}Zn ($T_{½}$ = 9.19 h) were determined non-destructively by γ-ray spectrometry, extrapolated to the end of bombardment (EOB) and corrected for various factors (see below) to obtain the decay rates. The decay-rate ratios of the above pairs were also calculated theoretically from the IAEA-recommended excitation functions of the reactions $^{nat}Cu(d,x)^{63}Zn$ and $^{nat}Cu(d,x)^{62}Zn$, respectively [4]. The mean energy of the deuteron beam effective in the front Cu foil was determined by comparing the experimentally obtained ratio with the theoretical one [12,13].

2.3 Beam flux monitoring

During each irradiation, the beam current was measured by charge integration. It gave only an approximate value. The deuteron flux effective in the samples was also determined by activation of Cu, Al and Ti monitor foils placed in front of a stack, whereby the $^{nat}Cu(d,x)^{62,63}Zn$, $^{27}Al(d,x)^{24}Na$ and $^{nat}Ti(d,x)^{48}V$ reactions served as monitors. From the measured decay rates of $^{62,63}Zn$, ^{24}Na and ^{48}V at EOB and their reference cross sections taken from the IAEA evaluated data file [4], the deuteron flux was determined. The individual flux values from the above monitors agreed within 6%. An average of those values was used to determine the cross section of the investigated reaction. This flux value was considered to be more accurate than that via charge integration. The computer program STACK written at Forschungszentrum Jülich (FZJ) and based on the energy-range relation [14], was utilized to calculate the beam energy degradation along the stack.

2.4 Measurement of radioactivity and analysis

The radioactivity of the investigated radionuclide was measured non-destructively using a high-purity germanium (HPGe) gamma-ray detector in combination with the necessary electronics and Maestro data acquisition software. The energy resolution (FWHM) of the HPGe detector used was 2.5 keV at 1332.5 keV γ-ray of ^{60}Co. The efficiency calibration of the detector was done using standard point sources, namely ^{54}Mn, ^{133}Ba, ^{137}Cs and ^{152}Eu, supplied by Isotope Products Laboratories. The uncertainty in the activity of each calibration source was specified as 3%. The γ-ray spectra were collected repeatedly in several time segments depending on the half-life of the radionuclide, and analyzed by the GammaVision and FitzPeaks [15] γ-ray peak analysis software.

The radioactivity of ^{28}Al ($T_{1/2}$= 2.246 min) and ^{27}Mg ($T_{1/2}$= 9.458 min) was measured about 5 min after the end of bombardment. Measurements were carried out at a distance of 50-60 cm from the detector surface to keep the dead time below 10%. The activity of the monitor product ^{24}Na in each target was measured for 5 min at a 20-50 cm distance, where both the true and random coincidence losses were negligible. The ^{24}Na activity measurement was started 4 h after the end of bombardment (EOB). The activity of the radionuclides ^{63}Zn and ^{62}Zn formed in a Cu monitor foil was measured for 5 -10 min after 2 h decay, and the counting position was 20-30 cm from the detector surface. In the case of the monitor product ^{48}V formed in Ti, the activity was measured about 48 h after EOB to allow complete decay of undesired short-lived products, and the measurement was performed for 1 h at a distance of 15 cm to obtain good counting statistics. The decay data of the investigated radionuclides were taken from the ENSDF Nuclear Database [16] and individual evaluations [17,18]. They are listed in Table 1.

2.5 Reaction cross section and its uncertainty

The peak area (counts) under a characteristic γ-ray of a reaction product was converted to count rate and extrapolated to the end of bombardment (EOB). This count rate was then converted to the decay rate by applying corrections for γ-ray intensity and efficiency of the detector. From this decay rate and the measured beam intensity, the cross section for the formation of the radioactive product was calculated using the well known activation equations.

The combined uncertainty in the cross section was estimated by taking the square root of the individual uncertainties in: peak area (1-7%), efficiency of the detector (5%), decay data, especially γ-ray intensities (0.01-0.07 %), half-life (0.08-0.13%) and deuteron flux (6 %). The overall uncertainty of measured cross sections amounted to 7-10% (1 σ).

3 Nuclear model calculation

The results of nuclear model calculations on products formed in deuteron-induced reactions are somewhat uncertain due to occurrence of direct interactions (breakup, stripping, etc.), in addition to the usual precompound and compound nucleus processes involved at energies of interest in this work. We made use of the TALYS-1.8 code, developed by Koning et al.[19] to calculate the cross sections of the reactions ^{27}Al(d,2p)^{27}Mg and ^{27}Al(d,p)^{28}Al. This code incorporates several nuclear models to calculate all the significant nuclear reaction mechanisms over the energy range of 1 keV to 200 MeV. In general, the results obtained for deuteron-induced reactions using global set of parameters, as expressed in the TENDL file [20], are not satisfactory. Special care regarding the choice of the input parameters is necessary to reproduce the experimental data. A few free parameters of the nuclear reaction models are optical model potential, level density formalism, spin distribution of the level density, γ-ray strength function, etc. As Pshiftadjust (adjustable pairing shift for adjustment of the Fermi Gas level density) we used the values of 1.0 and -1.5 for ^{28}Al and ^{27}Mg, respectively. These values are within the recommended limits [21]. The spin distribution of the level density was characterized by the ratio of the effective moment of inertia to the rigid-body moment of inertia ($\eta = \Theta_{eff}/\Theta_{rigid}$). For the best fitting of our ^{27}Mg data η=1.06 was used and for ^{28}Al, η value of 1.16 was used. Those values were obtained from the systematics based on the evaluation by Sudár and Qaim [22].

4 Results and discussion

4.1 ^{27}Al(d,αp)^{24}Na reaction: Validation of experimental techniques

We measured the excitation function of the ^{27}Al(d,αp)^{24}Na monitor reaction in two independent experiments to validate experimental techniques. We chose this reaction because of two reasons:

a) It is formed from the same target nucleus ^{27}Al as the other reactions under investigation.

b) The recommended data for this reaction have been provided by the IAEA after performing a critical evaluation of a large number of data sets produced by a large number of groups over the world [4].

A comparison of our experimental values with the recommended values should therefore vividly reveal the degree of agreement or deviation. The data obtained in the present work and the IAEA-recommended values are shown in Fig.1. The agreement between our data and the recommended curve over the whole investigated energy range is quite good and this fact gives high confidence to our measurements; it demonstrates that the various techniques used in this work at LBNL, especially the efficiency determination of the γ-ray counting system and the energy and intensity measurement of the deuteron beam, are reliable. It should be pointed out that up to deuteron energies of 37 MeV encountered in this work, the product ^{24}Na is formed only via the ^{27}Al(d,αp) reaction. At higher energies, the ^{27}Al(d,3p2n)^{24}Na process (E_{th}= 36.164 MeV) may also be involved. The IAEA-recommended curve is denoted as ^{27}Al(d,x)^{24}Na because it extends up to 80 MeV.

4.2 ^{27}Al(d,2p)^{27}Mg reaction

The experimental data and the results of the model calculation for this reaction are depicted in Fig. 2. Bém et al. [5] and Lebeda et al. [9] reported cross sections of this reaction up to 20 MeV. Below 17 MeV Wilson et al.[8] reported two data points. Those three data sets agree well with our experimental data, except in the region of 19 to 20 MeV where our values are about 15% lower. Beyond 20 MeV the data by Ochiai et al.[6] are significantly higher than our measured data. The experimental data of Radicella et al.[7] are scattered. Our data are reproduced well by the model calculation based on the code TALYS -1.8.

The (d,2p) reaction occurs possibly in two different ways: either the whole deuteron is absorbed to form an intermediate nucleus and thereafter two protons are sequentially evaporated, or more probably, at first stripping of the deuteron takes place that leads to the formation of an intermediate excited nucleus, which then disintegrates with the evaporation of a proton. A thorough theoretical analysis done by Bém et al.[5] showed that all processes contribute. Their global calculation using the code TALYS-1.0, however, gave rather high values. Furthermore, for a complete description of the (d,2p) reaction product, it is necessary to consider also the possible effect of the neutrons from the breakup process which may involve interactions with the target nucleus. A rather large amount of ^{27}Mg formed via the (n,p) reaction on ^{27}Al (E_{thr}= 1.896 MeV) before the effective threshold of the (d,2p) reaction may well correspond to the lowest energies of the breakup neutron [23] interacting with the target nucleus. However, practically no peak for the ^{27}Mg was observed in the gamma-ray spectrum of the activated Al foils placed at the end of a stack where the effective energies of the incident deuteron beam were below 6 MeV. Furthermore, the agreement of the measured cross sections of the (d,2p) reaction with the theoretically calculated cross sections using the code TALYS-1.8 is quite good, suggesting that the contribution of the d-breakup neutrons to the formation of ^{27}Mg is negligible.

4.3 $^{27}Al(d,p)^{28}Al$ reaction

The measured cross sections of this reaction are presented in Fig. 3 together with the results of the model calculation using the code TALYS-1.8. Four individual data sets available in the literature [5,8,10,11] are also shown in Fig. 3. They are scattered. Our data from two independent measurements are not exhaustive but are consistent. The data set by Bém et al. [5] is about 40% larger compared to our data in the overlapping energy range between 7 and 20 MeV. Considering the data of Schuster and Wohlleben [10] up to 3.2 MeV and our measurement and model calculation, it seems that the data by Bém et al.[5] have an energy shift of about 2 MeV upward. It is also likely that the values of Bém et al. are simply too high in the energy range of 6 to 16 MeV. No simple explanation could be found for this discrepancy because a fairly good agreement exists between Bém et al. and our data for ^{27}Mg and ^{24}Na formed in the same thin target. On the other hand, the systematic overestimation of data of Bém et al. may be the result of some missing common parameter in the determination of the cross section of this reaction, e.g. the efficiency of the detector or decay time which has serious effect in the case of the short-lived ^{28}Al compared to ^{27}Mg and ^{24}Na. The data reported by Wilson et al.[8] are much higher than other experimental data. Their value of 1000 mb at 6.75 MeV is certainly erratic. On the other hand, their data for the $^{27}Al(d,2p)^{27}Mg$ reaction are consistent with the other data. So the discrepancy is really in the case of the product ^{28}Al. Beyond 7 MeV the cross-section values of Flores [11] agree very well with our data. Their data from threshold up to 6.6 MeV are, however, not comparable with other experiments as well as with the model calculation. Flores [11] found the peak value of the excitation function between 7 and 8 MeV which appears to be incorrect. The precise experimental cross-section data of Schuster and Wohlleben [10] from 0.65 to 3.2 MeV (i.e. from threshold to maximum) agree well with the nuclear model calculation presented here, which also describes very well our measured data in the higher energy region. Thus we believe that the discrepancies in the existing data have been removed and the database has been strengthened up to 37 MeV.

It should be pointed out that the deuteron breakup process could also have a significant effect on the formation of ^{28}Al. The secondary neutron flux generated within the stack may induce the $^{27}Al(n,\gamma)^{28}Al$ reaction which leads to the same product as the (d,p) reaction. However, we estimated this contribution to be negligible because the thermal and fast neutron capture cross sections of ^{27}Al are small [24,25] and the expected neutron flux is also rather low.

4.4 Comparison of (d,αp) and (d,2p) reaction cross sections

A comparison of the cross sections of the ^{27}Al(d,αp)^{24}Na and ^{27}Al(d,2p)^{27}Mg processes appears interesting because in both cases two charged particles are emitted, in the former an α-particle and a proton, and in the latter two protons. A ratio of their cross sections is depicted in Fig. 4. The cross sections of both reactions were measured under the same experimental conditions. The ratio increases with the increasing incident projectile energy, reaches the maximum value at about 25 MeV, with no significant change thereafter. The ratio is less than 1 below 13 MeV, which means the ^{27}Al(d,2p)-process is stronger, possibly due to its lower reaction threshold of about 8.5 MeV than that of the ^{27}Al(d,αp)-reaction of about 10 MeV, as well as due to significant contribution of the stripping process. Above 13 MeV, however, the (d,αp) cross section increases sharply as compared to the (d,2p) process. It is postulated that after the stripping process, the probability of disintegration of the excited intermediate nucleus has a large preference for the emission of a complex particle compared to a single proton. This tendency appears to increase with the increasing projectile energy, resulting in the higher (d,αp) cross section. A yet another postulate may also be valid. Detailed nuclear model calculations by Bém et al.[5] suggest that in the formation of the ^{27}Al(d,p)^{28}Al reaction product, the stripping and evaporation contributions are approximately equal. The cross section of the ^{27}Al(d,α)^{25}Mg reaction [26], on the other hand, is about half of the (d,p) process. An analysis suggests [5] that the major contribution to α-particle emission is furnished by precompound/compound nucleus evaporation. Following the (d,p) and (d,α) interactions, the second chance emission in both cases then relates to a proton. Its emission probability appears to be higher after the first chance α-particle emission, and this probability increases with the increasing incident energy of the deuteron. It should, however, be clearly stated that activation experiments only allow to formulate some postulates. For a clear understanding of reactions involving emission of two charged particles, detailed physical experiments involving angular and energy distribution measurements of the emitted particles are needed.

5 Conclusion

New cross-section data sets of the reactions ^{27}Al(d,2p)^{27}Mg and ^{27}Al(d,p)^{28}Al were obtained by the activation technique up to deuteron energies of 37 MeV. The nuclear model calculations using the code TALYS-1.8 described our data well for the reaction products ^{27}Mg and ^{28}Al after modification of a few free input parameters within their recommended limits. From the cross-section ratios for the (d,αp) and (d,2p) processes as a function of projectile energy, deduced from their measured data, a large preference for the α-particle emission compared to the proton in the disintegration of the excited intermediate nucleus is postulated. An other postulate is that after the precompound/compound nucleus evaporation of an α-particle, the second chance emission of a proton has higher preference than that after the stripping process. Detailed angular and energy distribution studies are needed to understand the sequential emission of two charged particles.

Acknowledgements

M.S. Uddin thanks the Lawrence Berkeley National Laboratory, USA, for inviting him as visiting scientist. He would also like to acknowledge the authorities of Bangladesh Atomic Energy Commission and Ministry of Science and Technology, Dhaka, Bangladesh, for granting leave of absence to conduct these experiments abroad. We wish to thank the operation staff of the 88-inch cyclotron, LBNL, for providing the deuteron beam. This work was performed under the auspices of the US Department of Energy by Lawrence Berkeley National Laboratory under Contract No. DE-AC02-05CH11231.

References

1. Hagiwara, M., Itoga, T., Baba, M., Uddin, M.S., Hirabayashi, N., Oishi, T., Yamauchi, T.: Experimental studies on the neutron emission spectrum and activation cross-section for 40 MeV deuterons in IFMIF accelerator structural elements. J. Nucl. Materials **329-333**, 218-222 (2004).

2. Hagiwara, M., Itoga, T., Baba, M., Uddin, M.S., Sugimoto,M: Experimental studies on deuteron-induced activation reactions on IFMIF accelerator structural elements. J. Nucl. Materials **417**, 1267-1270 (2011)**.**

3. Bardayan, D.W.: Transfer reactions in nuclear astrophysics. J. Phys. G: Nucl. Part. Phys. **43**, 043001(2016).

4. Hermanne, A., Ignatyuk, A.V., Capote, R., Carlson, B.V., Engle, J.W., Kellett, M.A., Kib´edi, T., Kim, G., Kondev, F.G., Hussain, M., Lebeda, O., Luca, A., Nagai, Y., Naik, H., Nichols, A. L., Nortier, F.M., Suryanarayana, S.V., Takács, S., Tárkányi, F., Verpelli, M.: Reference cross sections for charged-particle monitor reactions. Nucl. Data Sheets **148**, 338-382 (2018).

5. Bém, P., Šimečková, E., Honusek, M., Fischer, U., Simakov, S.P., Forrest, R.A., Avrigeanu, M., Obreja, A.C., Roman, F.L., Avrigeanu, V.: Low and medium energy deuteron-induced reactions on ^{27}Al. Phys. Rev. C **79**, 044610 (2009).

6. Ochiai, K., Nakao, M., Kubota, N., Sato, S., Yamauchi, M., Ishioka, N.H., Nishitani, T., Konno, C.: Deuteron induced activation cross section measurement for IFMIF. Int. Conf. on Nuclear Data for Science and Technology, Nice 2007, France, Editors: O. Bersillon, F. Gunsing, E. Bauge, R. Jacqmin, S. Leray, EDP Sciences ,Vol.**2**, p.1011.

7. Radicella, R., Rodriguez, J., Baró, G.B., Hittmair, O.: Yield of nuclear reaction ^{27}Al(d,2p)^{27}Mg. Zeitschrift für Physik **150**, 653 (1958).

8. Wilson, R.L., Frantsvog, D.J., Kunselman, A.R., Détraz, C., Zaidins, C.S.: Excitation functions of reactions induced by ^{1}H and ^{2}H ions on natural Mg, Al and Si. Phys. Rev. C **13**, 976 (1976).

9. Lebeda, O., Štursa, J., Ráliš, J.: Experimental cross-sections of deuteron-induced reactions on ^{89}Y up to 20 MeV; comparison of ^{nat}Ti(d,x)^{48}V and ^{27}Al(d,x)^{24}Na monitor reactions. Nucl. Instrum. Methods Phys. Res. B **360**, 118 (2015).

10. Schuster, E., Wohlleben, K.: Activation analysis with deuterons: the total cross section of the reaction ^{27}Al(d,p)^{28}Al from 0.6 to 3.2 MeV. Appl. Radiat. Isot.**19**, 471(1968).

11. Flores, J.M.: Excitation function of the ^{27}Al(d,p)^{28}Al reaction between 2.2 and 12.6 MeV. Phys. Rev. **127**, 1246 (1962).

12. Piel, H., Qaim, S.M., Stöcklin, G.: Excitation functions of (p, xn) reactions on ^{nat}Ni and highly enriched ^{62}Ni: possibility of production of medically important radioisotope ^{62}Cu at a small cyclotron. Radiochim. Acta **57**, 1 (1992).

13. Uddin, M.S, Chakraborty, A.K., Spellerberg, S., Shariff, M.A., Das, S., Rashid, M.A., Spahn, I., Qaim, S.M.: Experimental determination of proton induced reaction cross sections on ^{nat}Ni near threshold energy. Radiochim. Acta. **104**, 305 (2016).

14. Williamson, C.F., Boujot, J.P., Picard, J.: Tables of range and stopping power of chemical elements for charged particles of energies from 0.5 to 500 MeV. Report CEA-R 3042 (1966).

15. Fitzgerald, J.: JF Computing Services, 17 Chapel Road, Stanford in the Vale, Oxfordshire, SN7 8LE. Copyright © Jim Fitzgerald 1991-2016, Last updated 8th October 2016.

16. ENSDF: Evaluated Nuclear Structure and Decay Data File, last updated on 2020-05-29, https://www.nndc.bnl.gov/ensdf/.

17. Basunia, M.S.: Nuclear data sheets for A= 27. Nucl. Data Sheets **112**, 1875-1948 (2011).

18. Basunia, M.S.: Nuclear data sheets for A= 28, Nucl. Data Sheets **114**, 1189-1291 (2013).

19. Koning, A.J., Hilaire, S., Duijvestijn, M.C.: TALYS-1.0. Proc .International Conference on Nuclear Data for Science and Technology, April 22-27, 2007, Nice, France, editors: O.Bersillon, F.Gunsing, E.Bauge, R.Jacqmin, and S.Leray, EDP Sciences, 2008, pp. 211-214.

20. Koning, A. J., Rochman, D., van der Marck, S. C., Kopecky, J., Sublet, J. Ch., Pomp, S., Sjostrand, H., Forrest, R., Bauge, E., Henriksson, H., Cabellos, O., Goriely, S., Leppanen, I., Leeb, H., Plompen, A., Mills, R.: TENDL-2019: TALYS-based evaluated nuclear data library. 31 December 2019.

21. Capote, R., Herman, M. , Oblozinsky, P., Young, P., Goriely, S., Belgya, T., Ignatyuk, A., Koning, A.J., Hilaire, S., Plujko, V., Avrigeanu, M., Chadwick, O.B.M., Fukahori, T., Kailas, S., Kopecky, J., Maslov, V., Reffo, G., Sin, M., Soukhovitskii, E., Talou, P., Yinlu, H., Zhigang, G.: RIPL 3 Reference Input Parameter Library for Calculation of Nuclear Reactions and Nuclear Data Evaluations. Nucl. Data Sheets **110**, 3107 (2009).

22. Sudár, S., Qaim, S.M.: Mass number and excitation energy dependence of the $\Theta_{eff}/\Theta_{rig}$ parameter of the spin cut-off factor in the formation of an isomeric pair. Nucl. Phys. A **979**, 113-142 (2018).

23. Qaim, S.M., Khatun, S., Wölfle, R.: Integral cross section measurements on (n,x) reactions induced by 30 MeV d(Be) breakup neutrons on FRT wall and structural materials. Proc. Symp. Neutron Cross Sections from 10 to 50 MeV, BNL-NCS-51245, pp. 536-552(1980).

24. Mughabghab, S.F., Garber, D.I.: Neutron Cross Sections. Vol. **1**, Resonance Parameters, BNL-325, 1973, and several later editions.

25. McLone, V., Dunford, C.L., Rose, P.F.: Neutron Cross Sections. Academic, New York, Vol. **2**, 1988.

26. Al-Quraishi, S.I., Brient, C.E., Grimes, S.M., Massey, T.N., Oldendic, J., Wheeler, R.: Low energy deuteron-induced reactions on ^{27}Al and ^{56}Fe. Phys. Rev. C **62**, 044616 (2000).

Figure captions:

Fig. 1. Comparison of experimental data with the IAEA-recommended curve for the $^{27}Al(d,\alpha p)^{24}Na$ monitor reaction.

Fig. 2. Comparison of experimental data with the model calculation for the $^{27}Al(d,2p)^{27}Mg$ reaction.

Fig. 3. Comparison of experimental data with the model calculation for the $^{27}Al(d,p)^{28}Al$ reaction.

Fig. 4. Ratio of cross sections of the (d,αp) and (d,2p) processes on ^{27}Al target as a function of deuteron energy.

Table 1: Decay data of the investigated radionuclides*.

Radionuclide	Production reaction	Q-value (MeV)	Half-life	γ-ray energy (keV)	γ-ray intensity (%)
^{24}Na	$^{27}Al(d,\alpha p)$	-5.36	14.997(12) h	1368.7	100
^{27}Mg	$^{27}Al(d,2p)$	-4.05	9.458(12) min	843.8	71.80(2)
				1014.5	28.20(2)
^{28}Al	$^{27}Al(d,p)$	5.50	2.245(2) min	1779.0	100

*Taken from the references [16,17,18].

Table 2: Measured cross sections for the formation of a few radionuclides in the ^{27}Al+d process.

.

Deuteron energy (MeV)	Measured cross sections of the products		
	^{24}Na	^{27}Mg	^{28}Al
36.6±0.4	34.8±2.7		18.3±1.6
34.7±0.4	38.1±2.8	12.3±1.1	
33.7±0.4	40.9±3.0	13.1±1.4	
31.8±0.4	43.3±3.1	14.2±1.5	
30.8±0.4	44.9±3.3	14.8±1.5	
29.0±0.4	50.2±3.7	16.4±1.2	
27.9±0.4	51.1±3.8	16.5±1.5	
27.7±0.4	54.9±4.3	17.5±1.3	44.9±4.1
25.5±0.4	57.2±4.1	17.6±1.8	
25.4±0.4	56.6±4.1	17.0±1.3	
24.3±0.4	58.4±4.2	18.0±1.3	
24.2±0.4	58.7±4.0	18.7±1.4	55.0±5.2
21.8±0.4	53.2±3.9	18.5±1.8	
21.6±0.4	54.5±4.0	18.7±1.4	
20.4±0.4	49.9±3.8	18.1±1.3	60.6±6.9
20.2±0.5	48.4±3.4	18.9±1.4	63.4±7.2
18.1±0.5	38.2±2.7	16.8±1.3	
16.5±0.5	26.8±2.0	14.1±1.1	
14.8±0.5	15.8±1.2	10.3±0.8	
13.0±0.5	6.3±0.6	6.8±0.5	97.8±12.2
12.9±0.5	6.0±0.5	5.8±0.6	
10.9±0.5	1.4±0.13	3.1±0.24	142.7±14.6
10.1±0.5	0.26±0.023	1.3±0.10	
9.9±0.5	0.22±0.025	1.5±0.13	154.6±16.7
7.3±0.5			241.1±28.3

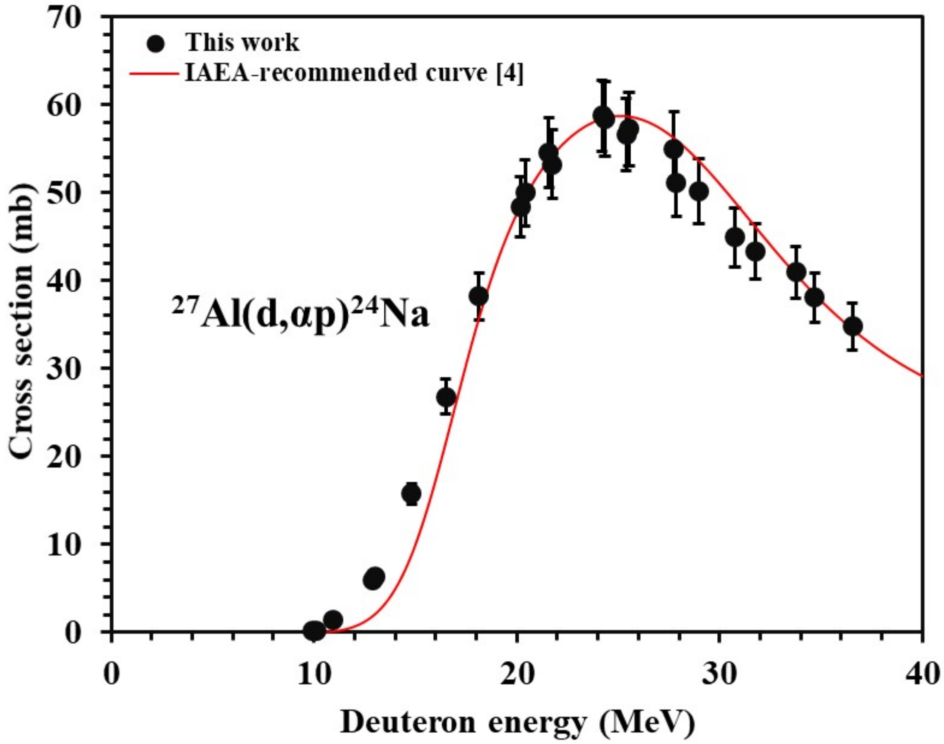

This work
IAEA-recommended curve [4]
$^{27}Al(d,\alpha p)^{24}Na$
Cross section (mb)
Deuteron energy (MeV)
0
10
20
30
40
50
60
70
0
10
20
30
40

Fig. 1

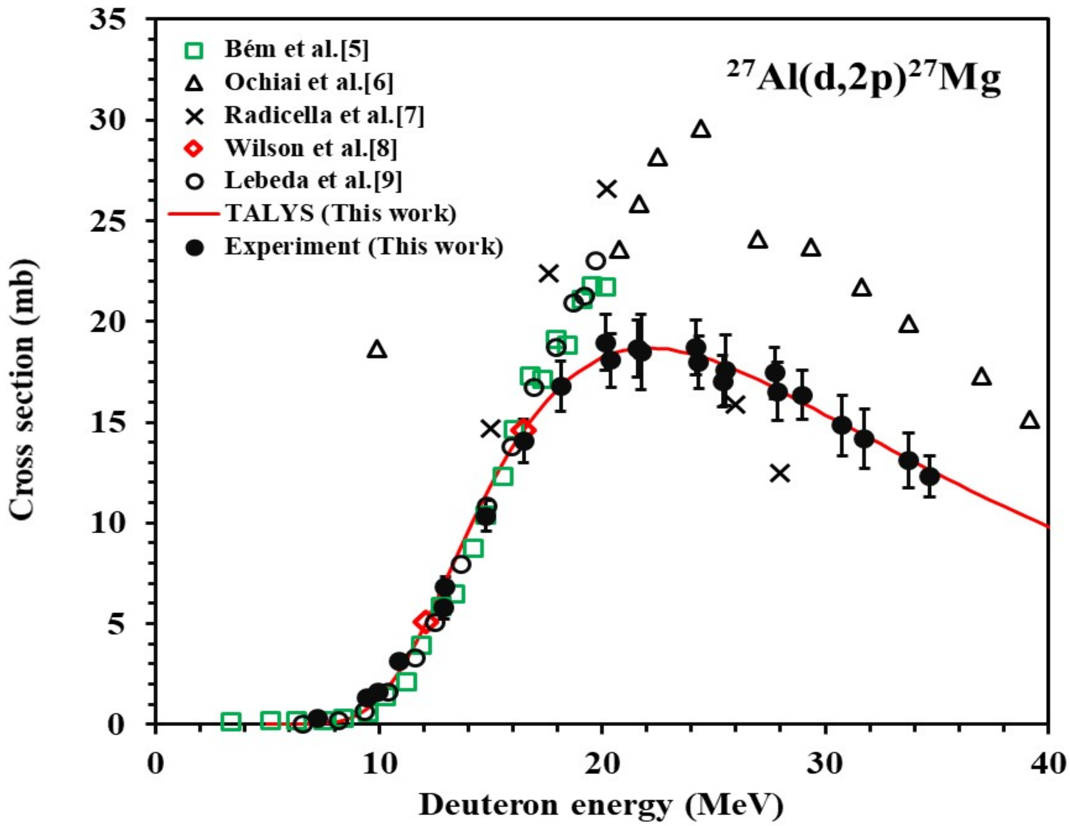

Bém et al.[5]
Ochiai et al.[6]
Radicella et al.[7]
Wilson et al.[8]
Lebeda et al.[9]
TALYS (This work)
Experiment (This work)
27Al(d,2p)27Mg
Cross section (mb)
Deuteron energy (MeV)
0
5
10
15
20
25
30
35
0
10
20
30
40

Fig. 2

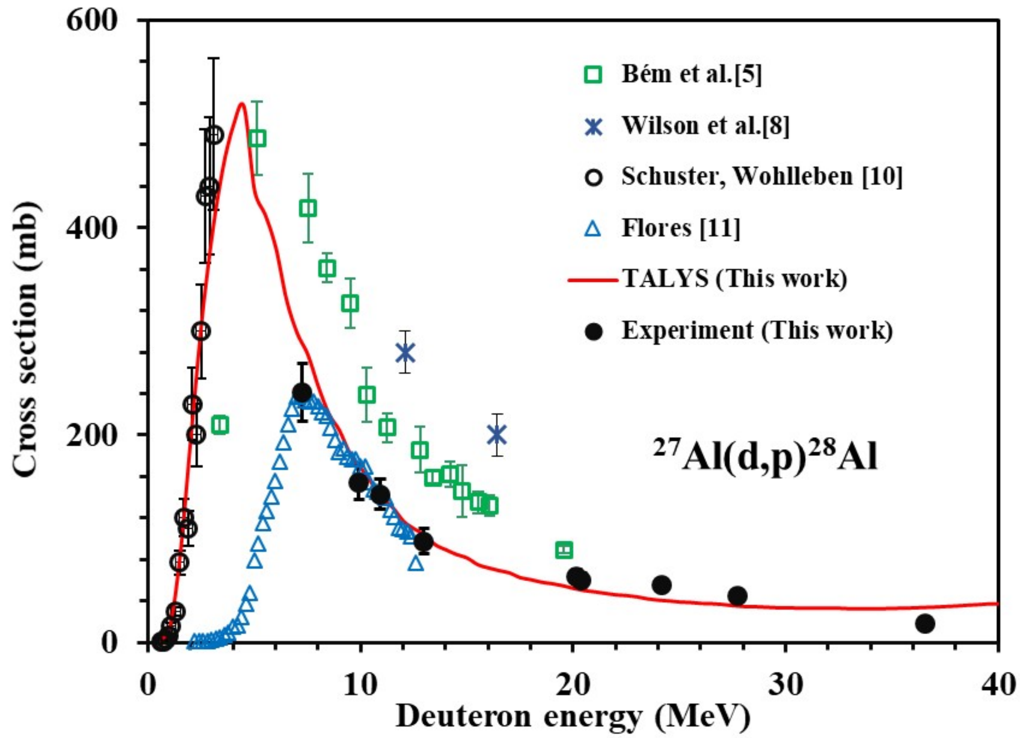
600
400
200
0
Cross section (mb)
0
10
20
30
40
Deuteron energy (MeV)
Bém et al.[5]
Wilson et al.[8]
Schuster, Wohlleben [10]
Flores [11]
TALYS (This work)
Experiment (This work)
$^{27}Al(d,p)^{28}Al$

Fig. 3

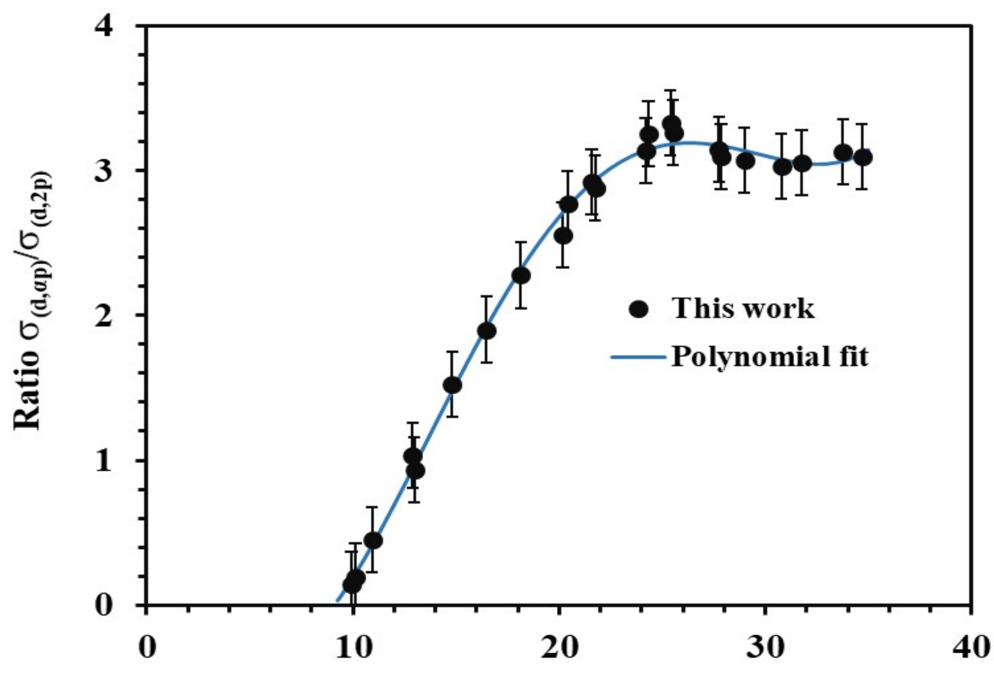
4
3
2
1
0
Ratio $\sigma_{(d,\alpha p)}/\sigma_{(d,2p)}$
0
10
20
30
40
Deuteron energy (MeV)
This work
Polynomial fit

Fig. 4